concluded as shown in Figure 6. L-Rha is just a mirror image of D-Man except for the replacement of a hydroxyl group on C6 by hydrogen. The structures of **1** and **2** are approximately mirror images of each other. Although D-Rib is a D-type aldose, the chelate skeleton structures and the absolute configuration of the asymmetric nitrogen of **3** are similar to those of **2**. These structural features seem to be in accordance with the CD spectral features.

Interestingly, the coordination behavior of *N*-glycosides formed from en and aldoses in the substitution-inert Co(III) system is greatly different from that in the substitution-labile Ni(II) systems[7,8] as follows: (i) The Co(III) complexes contain only one *N*-glycoside ligand. (ii) The sugar units bind to the Co atom at the three points of the donor atoms on C1, C2, and C3. (iii) The metal bindings induce structural changes in the sugar units.

The three-point binding through donor atoms on C1, C2, and C3 plays an essential role in terms of the polynuclear structure exhibited by the calcium complex with β-D-mannofuranose.[3] The same mode of binding is observed in the binuclear Ni(II) complex containing a β-D-mannofuranose derivative.[11] The stabilization of these complexes seems to be due to the binding of the metal–metal centers supported by the hydroxyl oxygens of the substituent group on C4. However, in the substitution-inert Co(III) complexes, their strong coordination bonds and the tetradentate chelation effects presumably contribute to the stabilization of the mononuclear complexes. In addition, Angyal et al. have reported the three-point interaction between alkaline-earth-metal ions and aldoses in aqueous solution.[2] It is of interest that the three-point binding is important in both the transition- and non-transition-metal complex systems; this contributes to a greater understanding of the interaction between metal ions and sugars.

Acknowledgment. We thank Prof. Kozo Sone and Prof. Yutaka Fukuda of Ochanomizu University for their helpful suggestions. We are grateful to Dr. Andrew C. Street for his helpful discussion. This work was partially supported by a Grant-in-Aid for Scientific Research from the Ministry of Education, Science and Culture of Japan (No. 63470035 and 63612002) and grants from Mitsubishi Foundation and Asahi Glass Foundation.

Cadmium Sulfide Mediated Photoelectric Effects in Bilayer Lipid Membranes

Subhash Baral and Janos H. Fendler*

Contribution from the Department of Chemistry, Syracuse University, Syracuse, New York 13244-1200. *Received May 27, 1988. Revised Manuscript Received October 6, 1988*

Abstract: Cadmium sulfide (CdS) particles, in situ generated on one side of glyceryl monooleate (GMO) bilayer lipid membranes (BLMs), have been used to mediate photoelectric effects. Steady-state and time-resolved photovoltage measurements have been carried out as functions of the wavelength and intensity of irradiation; variable current drain (external resistance); added electron donors and acceptors like methylviologen (MV^{2+}), K_2PtCl_6, $CuCl_2$, $KMnO_4$, $NaHSO_3$, $Na_2S_2O_5$, and KI_3; and the amount of oxygen present in the solution bathing the BLM. Steady-state illumination of a CdS-containing BLM resulted in the prompt development of −150 to −200 mV (the CdS or the cis side being negative) potential difference in an open circuit across the GMO BLM. This initial photovoltage, V_I, quickly decayed to a steady value, V_S (−100 to −150 mV). When the illumination was turned off, the potential difference across the GMO BLM decreased to its dark value in 3–4 min. Both V_I and V_S increased with increasing light intensities to saturation levels and produced action spectra corresponding to that of bulk crystalline CdS. Decreasing the concentration of oxygen in the solution bathing the BLM (by the addition of glucose, glucose oxidase, and catalase or by argon bubbling) reduced both V_I and V_S. Addition of electron scavengers to the cis side of the BLM increased the photovoltage. Conversely, photovoltage was reduced by the addition of hole scavengers to the cis side or by the removal of SH^- or H_2S from the side opposite to CdS (the trans side) of the BLM. Excitation of the CdS-containing GMO BLM by 20 ns, 353.4 nm laser pulses resulted in a transient photovoltage signal whose buildup fitted a single exponential ($t_{1/2} \sim 235 \pm 15$ ns) and whose decay could be resolved into a faster (complete within 40 μs) and a slower (complete within 1–2 s) component. The effect of additives was qualitatively similar to those observed in steady-state illuminations. Good linear current–applied voltage behavior was observed for the CdS GMO BLM both in the dark and under constant illumination. Slopes of these plots, 1.6 and 4.6 pA/mV, gave 6.3×10^8 and 2.2×10^8 ohms resistances in the dark and under illumination, respectively. The observed photoelectric effects have been rationalized in terms of equivalent circuits and chemical reactions. The chemical reactions included the following: band gap excitation of CdS to produce conduction band electrons, e_{CB}^-, and valence band holes, h_{VB}^+; reactions of trapped electrons, $e_{CB(t)}^-$, with oxygen at the semiconductor water interface ($O_{2(i)} + e_{CB(t)}^- \rightarrow O_2^{\bullet -}{}_{(i)}$); the diffusion of $O_2^{\bullet -}{}_{(i)}$ to the solution ($O_2^{\bullet -}{}_{(i)} + O_{2(s)} \rightarrow O_2^{\bullet -}{}_{(s)} + O_{2(i)}$); and oxidation of H_2S or SH^- by trapped holes, $h_{VB(t)}^+$ ($H_2S + h_{VB(t)}^+ \rightarrow HS^\bullet + H^+$ and/or $SH^- + h_{VB(t)}^+ \rightarrow HS^\bullet$). Thus, generation of $O_2^{\bullet -}$ in the cis and H^+ in the trans side of the solution bathing the CdS GMO BLM is the net consequence of bandgap excitation and the appearance of photovoltage is the result of vectorial transfer of charges in the direction opposite to and enhanced by the asymmetric membrane potential. Photovoltage decay is ascribed to charge recombination via mass transport of the ions through the BLM. These results have been compared to those reported previously on using "pigmented" BLMs.

A bimolecular thick membrane, a BLM, physically separates two aqueous solutions.[1,2] In the absence of additives or fortuitous impurities, the BLM is an excellent electrical insulator. Incorporation of ionophores or reconstitution of transport proteins into BLMs has increased ion conductivities across the membranes.[3-5] Sensitive electrical measurements in these systems have significantly contributed to our current understanding of the biological transport mechanisms.[6]

(1) Fendler, J. H. *Membrane Mimetic Chemistry*; Wiley-Interscience: New York, 1982.
(2) Tien, H. T. *Bilayer Lipid Membranes (BLM). Theory and Practice*; Marcel Dekker: New York, 1974.
(3) Miller, C. *Ion Channel Reconstitution*; Plenum: New York, 1986.
(4) Hille, B. *Ionic Channels of Excitable Membranes*; Sinaver Associates: Sunderland, MA, 1984.
(5) Sakmann, B.; Neher, E. *Single-Channel Recording*; Plenum: New York, 1983.

0002-7863/89/1511-1604$01.50/0

Similarly, measurements of photoelectric effects in appropriately "pigmented" BLMs have provided some insight into such light-initiated processes as photosynthesis and vision.[7,8] Chlorophylls, porphyrins, and dyes have been used as pigments. More recently, microcrystalline, metallic, magnetic, and semiconducting particles and films have been in situ generated in BLM surfaces.[9-12] These particles, initially appearing as dots on the BLM surface, rapidly moved around and grew in size, forming islands that merged with themselves and with successive generations of dots. Ultimately, the coalescing particles produced a film that considerably stabilized the BLM. Particle formation on BLMs has been monitored and characterized by simultaneous electrical and intracavity laser absorption,[13] fluorescence,[14] reflection,[11] and surface-enhanced resonance Raman (SERRS)[15] spectroscopic techniques. The obtained data, treated in terms of an equivalent R-C circuit, led to a morphological description of the BLM-incorporated particles and films.[11,15]

Development of semiconductor- and magnetic-particle-containing BLMs has been prompted by the mimetic relevance of these systems. In particular, we have been interested for some time in artificial photosynthesis.[16] Optimization of a given system requires an understanding of the mechanisms of photoelectron transfers in the environments of, and across, mimetic membranes. We have undertaken, therefore, a systematic study of semiconductor-mediated photoelectric effects in BLMs. The present article reports results on steady-state and time-resolved, cadmium sulfide mediated photovoltage and photocurrent measurements in glyceryl monooleate BLMs.

Experimental Section

Chemicals. Glyceryl monooleate (GMO) was obtained from Nuchek Preparations, Inc. The BLM-forming solution was made by diluting 50.0 mg of the lipid (as received) with 1.0 mL of dry decane (+99% purity, Aldrich Chemical Co.). The stock solution was kept in the refrigerator at −5 °C and a small amount (about 200 μL) was taken out at a time for 1 week's use. $CdCl_2$, $CuCl_2$, KI, I_2, $KMnO_4$, $NaHSO_3$ (Baker Analysed Reagents), $Na_2S_2O_5$ (Sigma Chemical Co.), D(+)-dextrose, glucose oxidase from penicillium amagasakienze (30 000 units/gm, United States Biochemical Co.), and purified catalase from bovine liver (4000 units/mg, Sigma Chemical Co.) were used as received. Methylviologen dichloride, chloroform, and ethanol were obtained from Aldrich Chemical Co. Water was purified with a Millipore Milli-Q system provided with a 0.4-μm Millistak filter at the outlet.

BLM Formation. A thin (100–150 μm) Teflon film containing a 0.1 cm diameter hole was sandwiched between two 1.0 cm pathlength quartz cells by silicone rubber adhesive. The faces of the two cells, in contact with the Teflon film, contained 0.6 cm × 1.5 cm windows through which the 0.1 cm diameter hole and some surrounding area of the Teflon film remained exposed. The cells were filled with 4 mL of 5 mM KCl solution at ambient temperature. The BLMs were made by brushing a small amount of the BLM-forming solution on the 0.1 cm diameter hole. Thinning of the initially formed thick film to a black bilayer lipid membrane was monitored by observing the reflected light from a 200 W mercury-xenon lamp through a microscope and by capacitance measurements. The accuracy of capacitance measurements was found to be within 1.0%.

Semiconductor Formation. Semiconductor formation on BLMs has been described previously.[11] Briefly, 100 μL of 0.2 M $CdCl_2$ solution was added to 2.0 mL of 5.0 mM KCl bathing solution on one side, hereinafter called the cis side, of the BLM followed by addition of 100 μL of 5.0 mM KCl on the other side, hereinafter called the trans side, to equalize the hydrostatic pressure across the BLM. After about 15 min of incubation, 160–200 μL of H_2S gas was slowly injected into the 5.0 mM KCl bathing solution on the trans side over a period of about 4–5 min. Within approximately 10 min, colorless CdS particles became visible on the BLM surface and soon the entire BLM surface became covered with yellow crystalline particles. Spectrophotometric studies show that the CdS formation was essentially complete (>80%) in about 2 h.[11]

Oxygen was removed, when required, by two different methods: (i) by prior bubbling of the bathing solution with argon gas for 30 min and subsequently maintaining an argon atmosphere around the BLM cell (by enclosing it in a box with a positive argon pressure) during the BLM formation, semiconductor deposition, and subsequent measurements; or (ii) by adding 26 μL each of 1 M D(+)-dextrose, glucose oxidase (10 mg/mL), and catalase (5 mg/mL) to the cis or both to the cis and trans sides of the BLM. Oxidation of glucose to gluconic acid by this enzyme–substrate combination has been shown to reduce the concentration of dissolved oxygen down to 10^{-7} M[17,20] and, thus, allows one to work in macroscopically anaerobic conditions in an open system. The catalase present efficiently destroys any hydrogen peroxide formed.

Photoelectrical Measurements. Either a 200 W mercury-xenon or a 250 W xenon lamp was directed to either side (i.e., to the CdS or to the hydrocarbon side) of the semiconductor-containing BLM by a glass (which cuts off the UV radiation at a wavelength less than 350 nm) optical fiber guide. The irradiation energy impinged on the BLM area was varied between 5.0×10^{-6} and 4.0×10^{-9} W by means of a series of neutral density filters. The steady-state photovoltage produced was measured with a Model 602 Keithley Electrometer (input impedance 10^{14} ohms shunted by 20 pF) connected to two identical Ag/AgCl electrodes dipped in the bathing solutions on opposite sides of the BLM. The positive input of the electrometer was connected to the electrode on the cis (CdS) side of the BLM. The other electrode was essentially grounded. The Ag/AgCl electrodes were covered with black Teflon sleeves to avoid the generation of any spurious photovoltage. All necessary precautions were taken to keep the illumination of the semiconductor-containing BLM to a minimum during the semiconductor deposition. Photovoltage measurements were done in complete darkness with only the light from the fiber guide falling on the BLM after the shutter was opened. The electrometer output (reversed for easier monitoring on the electrometer panel) was fed to a Y-t recorder for continuous recording. The magnitude of the photovoltage was measured as the change in the potential difference across the two Ag/AgCl electrodes between the dark and illuminated states. Photovoltage measurements usually commenced about 90–120 min subsequent to H_2S injection. This waiting period was necessary to ensure that the baseline (potential difference across the electrodes in the dark) did not drift significantly during the course of an experiment. Also, the change in photovoltage with time after this induction period became negligibly small (vide infra). The experimental procedures routinely included careful checking of the photovoltages (i) in the absence of semiconductor on the BLM, (ii) in the absence of illumination, and (iii) in the absence of a BLM.

The experimental setup for recording photovoltage action spectra consisted of a 200 W mercury-xenon lamp, a Jarrell-Ash 82-410, 0.25 m Ebert monochromator, a pair of Ag/AgCl electrodes, and the Keithley Model 602 electrometer. The illumination band width for the slit widths used was 20 nm. An additional light source (a 250 W xenon lamp and an optical fiber guide) was used to monitor BLM formation and semiconductor deposition. This lamp was turned off during photovoltage measurements. The photovoltage action spectra was measured by rotating the grating inside the monochromator manually, point-by-point, in increments of 20 nm and measuring the voltage change on illumination at each point. The photovoltages measured at different wavelengths were then corrected for the variation in lamp power at different spectral regions. The light energy was measured using a Scientech Model 36-2002 power meter for pulsed illumination and a Spectra Physics Model 404 photodiode for steady-state measurements. A mask with a circular hole of approximately the area of the bilayer lipid membrane was used at the

(6) Hoppe, W.; Lohmann, W.; Markl, H.; Ziegler, H. *Biophysics*; Springer: New York, 1983.
(7) Tien, H. T. In *Photosynthesis in Relation to Model Systems*; Barber, J., Ed.; Elsevier/North Holland Biomedical Press, 1979; pp 116–172. Tien, H. T. *Progr. Surf. Sci.* **1986**, *23*(*4*), 317–412.
(8) Hong, F. T. *Photochem. Photobiol.* **1976**, *24*, 155–189.
(9) Baral, S.; Zhao, X. K.; Rolandi, R.; Fendler, J. H. *J. Phys. Chem.* **1987**, *91*, 2701–2704.
(10) Kutnik, J.; Tien, H. T. *Photochem. Photobiol.* **1987**, *46*, 413–416.
(11) Zhao, X. K.; Baral, S.; Rolandi, R.; Fendler, J. H. *J. Am. Chem. Soc.* **1988**, *110*, 1012–1024.
(12) Zhao, X. K.; Herve, P. J.; Fendler, J. H. *J. Phys. Chem.*, in press.
(13) Zhao, X. K.; Fendler, J. H. *J. Phys. Chem.* **1986**, *90*, 3886–3890.
(14) Rolandi, R.; Flomm, S. R.; Dillon, I.; Fendler, J. H. *Prog. Colloid Polym. Sci.* **1987**, *73*, 134–141.
(15) Zhao, X. K.; Fendler, J. H. *J. Phys. Chem.*, in press.
(16) Fendler, J. H. *J. Phys. Chem.* **1985**, *89*, 2730–2740.
(17) Ilani, A.; Liu, T. M.; Mauzerall, D. *Biophys. J.* **1985**, *47*, 679–684.
(18) Everitt, C. T.; Haydon, D. A. *J. Theor. Biol.* **1968**, *18*, 371–379.
(19) Kutnik, J.; Tien, H. T. *Photochem. Photobiol.* **1987**, *46*, 1009–1013.
(20) Concentration of dissolved oxygen was monitored by measuring the cathodic current due to the reduction of dissolved oxygen at −0.175 V (SCE). Addition of enzyme mixtures brought the cathodic current down from 20 to 0.2–0.3 mA within 3 min. In solutions containing 2.0×10^{-3} M K_2PtCl_6 (in addition to the enzyme mixture) the rate of oxygen depletion was observed to be the same. Therefore, K_2PtCl_6 does not inhibit or oxidize glucose oxidase or catalase.
(21) Instability of the electric components used did not allow the monitoring of the slower decays to completion. No kinetic constants were calculated, therefore, for the slow component of the photovoltage decays.

entrance of the power meter positioned in the same plane as the BLM. A set of neutral density filters were used to control the illumination intensity.

For photocurrent measurements, the Keithley Model 602 electrometer was used in the current-measuring mode in which the potential drop across an external resistor shorting the two Ag/AgCl electrodes was measured. By varying the magnitude of this external resistance, the dependence of the steady-state photovoltage on the current drawn from the CdS-BLM photocell can be determined. The short circuit photocurrent was measured using a Dagan Model 8900 patch clamp connected to the pair of Ag/AgCl electrodes via a 8910 probe (0.1 GΩ resistance in the feedback circuit) and clamping the potential difference between the two electrodes at 0 V. By clamping this potential at different values and measuring the change in the feedback current on illumination, a photocurrent–potential curve for the CdS-BLM photocell could be constructed.

Time-resolved photovoltage measurements were done by connecting the pair of Ag/AgCl electrodes to a Tektronix Model 7834 storage oscilloscope (the electrode on the cis side to +ve input) via a 10× probe. The presence of a 10× probe, although cutting down on the signal amplitude, improves the time response of the measuring system. With a wideband filter, the time constant of the measuring system, including a BLM or an electronic equivalent of BLM, was found to be <50 ns from the measurement of the risetime of a square wave pulse. Pulsed irradiation was done with use of 20 ns laser pulses from the third (353.4 nm) harmonics of a Quanta Ray DCR-1 ND-YAG laser. The laser beam of typical energy 2×10^{-3} mJ (using neutral density filters to attenuate the 2–10 mJ energy of the beam) with a spot area almost the same as the BLM area was obtained by focusing the laser at the center of the BLM with a plano-convex lens of 50 cm focal length. It should be noted that, in the steady-state measurements, the inputs were inverted by the electrometer before being recorded, but no such inversion occurred in the time-resolved measurements. Hence, a steady-state photovoltage signal going upward has the same polarity as that of a time-resolved signal going downward.

Results and Discussion

Resistance and Capacitance Measurements. Prior to CdS deposition, the resistance and the capacitance of a typical GMO BLM was determined to be (3–5) × 10^8 ohms and 2.0–2.2 nF. These values are in good agreement with those expected for a BLM of 0.07–0.08 cm diameter.[2] Subsequent to the completion of CdS formation on the GMO BLM (about 2 h after the addition of reactants to the bathing solutions), the resistance and capacitance across the semiconductor-containing BLM were found to be reduced to (1–5) × 10^8 ohms and 1.5–1.8 nF, respectively. This lowering in resistance and capacitance has been attributed to partial penetration of the BLM by the semiconductor particles on one surface.[11]

Steady-state irradiation of a CdS-containing GMO BLM resulted in a further decrease in resistance to about (0.5–3.0) × 10^8 ohms. Usually the observed resistance drop was in the range of 20–25% with any particular CdS GMO BLM (resistances could be measured reproducibly with ±5% accuracy). Absence of an appreciable resistance change across the semiconductor-containing BLM upon steady-state irradiation is accountable in terms of incorporation of CdS into, rather than a fully spanned penetration across, the GMO BLM. However, there was a slight increase in capacitance (about 5–10%) upon irradiating a CdS-containing GMO BLM. The capacitance of a BLM could be measured within 1%.

The BLM, as a first approximation, can be considered to be equivalent to a parallel plate capacitor immersed in a conducting bathing solution.[8,18] Figure 1a shows the equivalent circuit describing the resistance (R_m) and the capacitance (C_m) of the BLM as well as the resistances (R) and capacitances (C) of the electrodes (indicated by subscript E) and those of the electrolytes in the solution (indicated by subscript S) at the cis (indicated by subscript 1) and the trans (indicated by subscript 2) sides of the membrane between two summing points (A and B). Usually C_{E1} and C_{E2} are larger than C_m and, thus, do not contribute significantly to the observed capacitance measured across the electrodes in the presence of a BLM. The contribution from the electrodes and electrolytes toward the observed photoelectric effect was found to be negligible as their electrical properties did not change during irradiation.

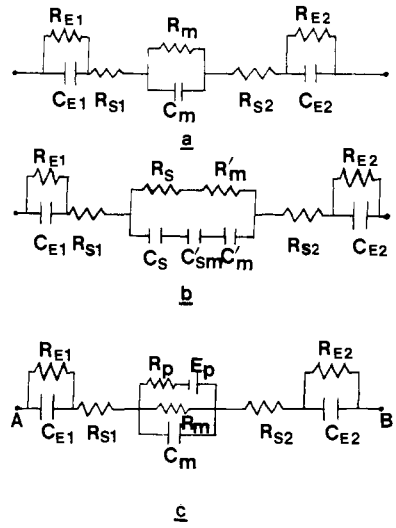

Figure 1. Equivalent circuit descriptions of a simple BLM (a); a CdS-containing BLM in the dark (b); and a CdS-containing BLM when irradiated (c).

Deposition of semiconductors on the BLM surface requires some modification of the circuit shown in Figure 1a. Simultaneous capacitance and reflection measurements provided morphological information on the semiconductor-containing BLM.[11] In particular, semiconductor particles were shown to penetrate the BLM[11] to a depth of no more than 18 Å and to grow to several hundred ångströms in thickness in the direction perpendicular to the plane of the BLM. This led to an equivalent circuit consisting of three series capacitors (that originating in the semiconductor electrolyte junction, C_S, in the composite semiconductor–hydrocarbon mixture, C'_{sm}, and in the hydrocarbon core of the BLM, C'_m) and two series resistors (that due to the semiconductor, R_s, and to the hydrocarbon core of the membrane, R'_m) in parallel (Figure 1b). Relationships between the two circuits (Figure 1, a and b) are given by

$$R_m = R_s + R'_m \tag{1}$$

$$\frac{1}{C_m} = \frac{1}{C_s} + \frac{1}{C'_{sm}} + \frac{1}{C'_m} \tag{2}$$

The model shown in Figure 1b describes remarkably well the electric properties of the CdS-containing GMO BLM in the dark (Figure 2). Thus, for example, the current–voltage behavior is given by the expression

$$I_d = \frac{(V_A - V_B) + \Phi_m}{R_m} \tag{3}$$

where I_d is the dark current through the membrane and also the feedback current when the membrane is held at a potential $V_A - V_B$, and Φ_m is the asymmetric membrane potential (arising from different solution compositions and, hence, from different surface charge densities on the different sides of the BLM). Analysis of the data in Figure 2 in terms of eq 3 led to $R_m = 6.3 \times 10^8$ ohms (from the slope) and $\Phi_m = +426$ mV (from the intercept). The asymmetric BLM potential Φ_m may be regarded as originating from differential charging of the capacitor C_m (i.e., when the clamped voltage across the BLM is equal to Φ_m, no feedback current is necessary in the voltage clamp circuit to hold, or clamp, that voltage).

Photovoltage Measurements. Subsequent to the CdS formation, a small potential difference (−30 to +10 mV) was measured in the open circuit between the Ag/AgCl electrodes across the BLM even in the absence of illumination. This potential difference, due to the asymmetry of the composition of the solutions bathing the BLM, could originate in the different solution compositions of the cis and trans side of the BLM, as well as in the alteration of the Ag/AgCl electrode by H_2S. In addition to the 5 mM KCl supporting electrolyte surrounding the BLM, the cis side contained unreacted $CdCl_2$, while H_2S and HS^- were present in the trans

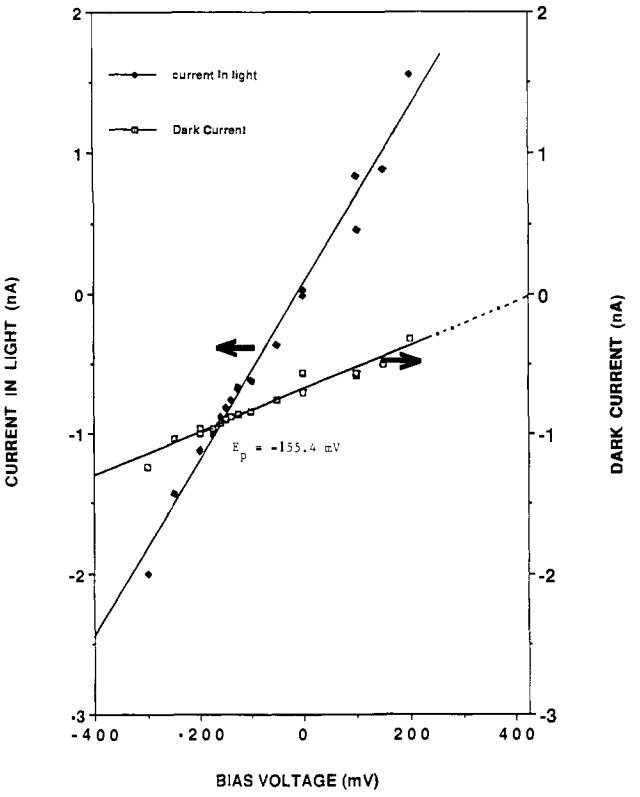

Figure 2. Current passing through a CdS-containing GMO BLM as a function of the potential difference held across the BLM with a patch clamp in the dark (open squares, □) and in the presence of light (4.0×10^{-6} W of energy incident upon the BLM, full squares, ■). The magnitude of the photocurrent at any voltage is given by the difference in the ordinate of the two points with the same abscissa (i.e., bias voltage).

side. The pH of the solution bathing the BLM was kept between 5.5 and 5.8. Under this condition, the predominant sulfur species present is H_2S (pK_a = 7.0 for H_2S/SH^-).

When the light shutter was opened, the potential difference across the BLM in the open circuit instantly reached a value between −150 and −200 mV, with the Ag/AgCl electrode on the cis side (the side of the BLM that contained the CdS particles) becoming negative. This initial photovoltage, defined as the change in the potential difference across the BLM by irradiation and designated as V_I, then quickly relaxed to a steady value, V_S (the electrode on the cis side still remaining negative). Over a short period of illumination, e.g., 5–10 min, the open circuit photovoltage magnitude remained constant at V_S. When the illumination was turned off, the observed potential difference across the BLM decayed to its dark value in approximately 3–4 min. Typical photovoltage signals from a CdS-containing GMO BLM was shown in Figure 3 (lower portion). Reproducibility of V_I and V_S values was determined to be within 10%.

Photocurrent Measurements as a Function of Potential Difference across the BLM. Steady-state photocurrents were also determined at different bias voltages applied across the CdS-containing BLM. Advantage was taken of the ability of the patch clamp to hold a potential difference across the BLM at a predetermined value in the +400 and −400 mV range. Beyond this range, the CdS-containing BLM was found to be unstable. Good linear current–applied voltage behavior was observed for the CdS GMO BLM, both in the dark and under constant illumination (Figure 2). The photocurrent at any particular voltage is given by the vertical difference between these two lines at that voltage. In the dark, the slope of the current–voltage curve was found to be small (1.6 pA/mV) corresponding to a composite resistance of the CdS-containing BLM (6.3×10^8 ohms). Upon illumination, the current–voltage slope increased to 4.6 pA/mV and the resistance decreased to 2.1×10^8 ohms. It is interesting to note that when the CdS-containing GMO BLM was held at a potential corresponding to the intersection of the two current–voltage curves

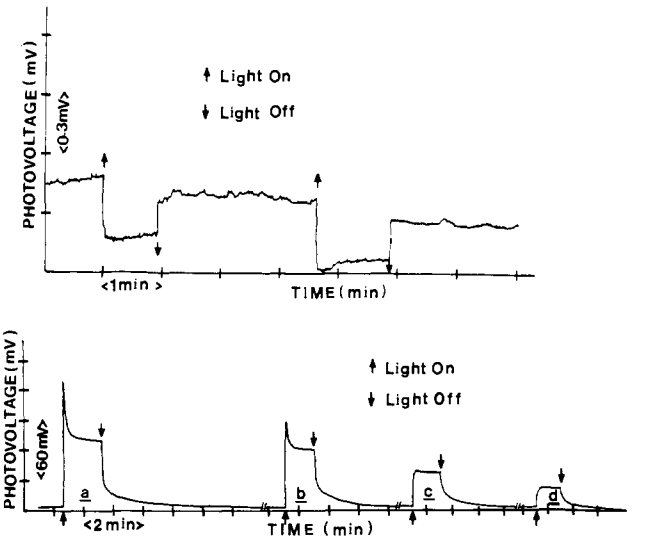

Figure 3. Photovoltage signals obtained from a CdS-containing GMO BLM when illuminated with a steady-state lamp with 4.08×10^{-6} W (a), 0.89×10^{-6} W (b), 0.042×10^{-6} W (c), and 0.033×10^{-6} W (d) energies incident upon the GMO BLM. The upper plot indicates results of irradiation of the electrode (with the Teflon sleeve removed) in the absence of CdS (see Results for experimental details).

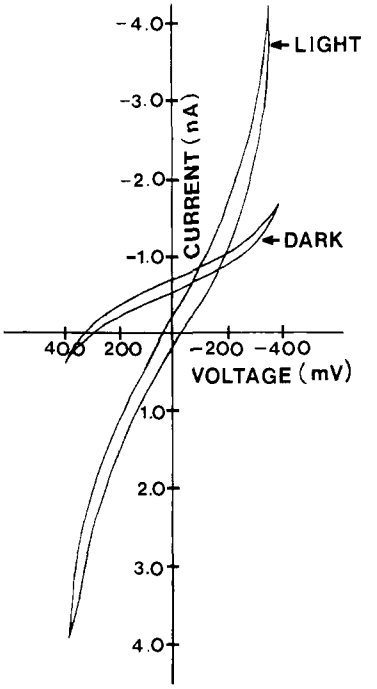

Figure 4. Cyclic voltammograms recorded for a CdS-containing GMO BLM in the dark and when illuminated with light of 4.0×10^{-6} W of energy incident upon the BLM.

(~150 mV), the observed photocurrent was zero at all light intensities. It is also interesting to note that for the irradiated BLM when the voltage is clamped at 0 V, the current passing through the BLM is also zero.

Cyclic voltammograms of CdS-containing GMO BLMs, in the dark and under illumination, are shown in Figure 4. The voltammograms were taken in a two-electrode configuration using a triangular voltage sweep (50 mV/min) as the command voltage input to the patch clamp. Once again, the I–V curve of the BLM under irradiation passes very close to the $I = 0$, $V = 0$ point (origin).

Steady-state illumination of the semiconductor-containing BLM could not be treated in terms of the simple circuits shown in Figure 1, a or b. The decreased resistance of the BLM, caused by the light, can be accommodated in a model equivalent circuit that

includes a photoconduction pathway through a resistor, R_p, in parallel with R_m (Figure 1c). The value of R_p is, of course, infinity in the dark and is a finite function of the intensity of the steady-state irradiation. Analysis of Figure 2 showed that, even under constant illumination, the observed photocurrent is an asymmetric, but linear, function of the potential difference held across the BLM by the patch clamp. This observation can be rationalized by introducing an emf source,[8] E_p, as in the circuit shown in Figure 1c. Once again, in the dark, the magnitude of the emf produced by the source is 0, while in the presence of light its value is a function of the light intensity. Thus, from Figure 1c, when R_{E2} and R_{E1} are small, the photocurrent, I_p, is given by

$$I_p = \frac{(V_A - V_B) + E_p}{R_p} \quad (4)$$

A similar equation has recently been applied to describe the photoelectric behavior of a metalloporphyrin-containing BLM.[19] When E_p is equal in magnitude, but opposite in sign, to $V_A - V_B$ (i.e., to the potential at which the BLM is held by the patch clamp between the two summing points, A and B) $I_p = 0$. Such point is given by the intersection of the dark and light current–voltage lines (see in Figure 2). From this intersection, E_p was found to be −155.4 mV for the CdS GMO BLM on which this experiment was performed. Slopes of these plots (Figure 2) also yielded $R_p = 2.17 \times 10^8$ ohms and $R_m = 6.28 \times 10^8$ ohms. Similar measurements on another CdS-containing GMO BLM, prepared at a different time, resulted in $R_m = 3.8 \times 10^8$ ohms, $R_p = 1.2 \times 10^8$ ohms, and $E_p = -184$ mV. These results indicate satisfactory consistencies between the different preparations. The E_p values (−155.4, −184 mV) also agree well with that determined in the open circuit photovoltage experiments under steady-state irradiations (120–150 mV). It is interesting to note that R_p values are several orders of magnitude larger than that expected had the BLM been shorted by complete penetration of the CdS particles.

Combining eq 3 and 4, the total feedback current during steady-state irradiation is given by

$$I_{light} = I_d + I_p = \frac{(V_A - V_B) + \Phi_m}{R_m} + \frac{(V_A - V_B) + E_p}{R_p} \quad (5)$$

From Figure 2, it can be seen that when $V_A - V_B = 0$, $I_{light} \approx 0$, so that we can write

$$E_p = -\Phi_m(R_p/R_m) \quad (6)$$

The values of $\Phi_m = +426$ mV, $R_m = 6.3 \times 10^8\ \Omega$, and $R_p = 2.2 \times 10^8\ \Omega$, give, on substitution in eq 6, $E_p = -147$ mV. This value is remarkably close to the observed open circuit photovoltage and also to the value determined from the intersection of the two lines shown in Figure 2 (−155.4 mV).

The relaxation kinetics of the photovoltage from V_I to V_S was found to be of single exponential over 3–4 half-lives. The relaxation rate appeared to be independent of the intensity of illumination. The first-order time constant of the relaxation, however, was found to vary from 10 to 30 s with different CdS-containing GMO BLMs. For any one CdS-containing BLM, however, the half-life was longer (30–50 s) at the very beginning of the experiments when the virgin semiconductor had been freshly exposed to light, but it quickly (after being exposed to light for a total of about 6–10 min) reached a steady value that did not subsequently change during further illumination cycles. Leaving the CdS-containing BLM at this point in the dark for a long time (45 min or longer) again resulted in a longer half-life. Illumination for about 10 min at this point, once again, brought the half-life in the 10–30 s range. The decay of photovoltage when the light was turned off was multiexponential, showing the presence of at least one fast and one slow component. The magnitudes of both the fast and slow components also seemed to be independent of illumination intensity. When a CdS-containing GMO BLM was left for about 48 h, it did not show any photovoltage on illumination. However, injection of about ~100 μL of H_2S on the trans side once again resulted in the development of photovoltage.

Effects of Light Intensity. When the intensity of the light falling on the CdS-containing BLM was increased above 4–5 × 10^{-6} W, a saturation effect of both V_I and V_S was observed. As the light intensity was reduced below 5 × 10^{-6} W, the magnitude of V_I dropped, but V_S remained virtually unchanged until the light intensity was about 1 × 10^{-6} W. Below 1 × 10^{-7} W, V_I and V_S became almost the same, i.e., $V_I - V_S \simeq 0$. Further reduction of the light intensity led to a linear decrease of V_I and V_S. These changes in the nature of the photovoltage signal with illumination intensity are illustrated in Figure 4 (lower curve). A plot of the magnitude of V_I and V_S vs the irradiation energy for a typical CdS-containing GMO BLM is shown in Figure 5 and inset. From Figures 3 and 5 it is also obvious that V_S saturates at much lower irradiation energy than V_I.

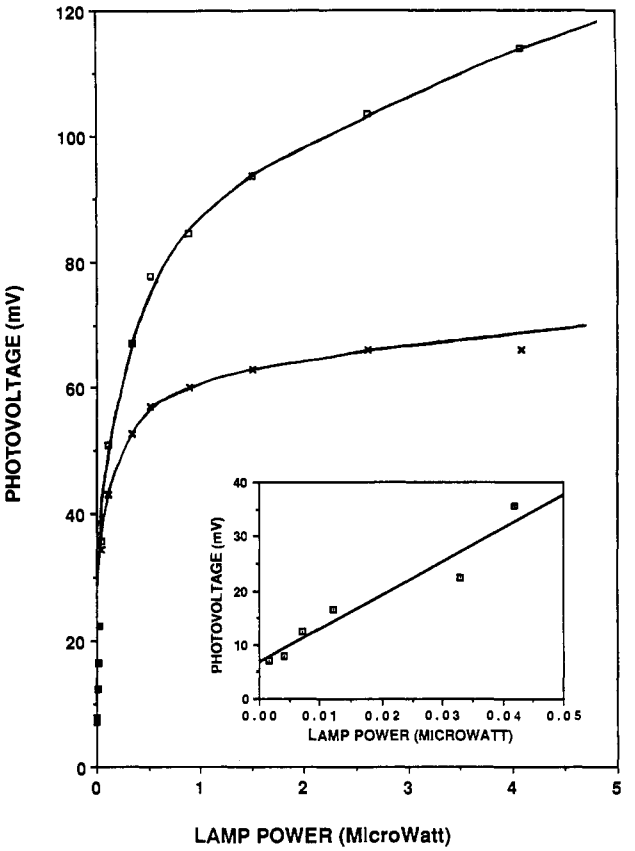

Figure 5. Plot of CdS photovoltage as a function of irradiation energy falling on the BLM surface. The low power region is expanded in the insert. Initial value, V_I (□), steady-state value, V_S (×). In the low power region, $V_I = V_S$.

Time Evolution of Photovoltage. A typical time evolution of photovoltage during the course of CdS deposition on a GMO BLM is shown in Figure 6. The first measurable (>1 mV) photovoltage appeared 20 min subsequent to the addition of the precursors. Following a modest increase in V_I and V_S, most of the growth in photovoltage occurred in the 40–60 min period subsequent to initiation of the CdS deposition. It is interesting to note that from the very beginning, both V_I and V_S developed in a very similar manner, paralleling the increase in the amount of CdS on the BLM. The initial drop in photovoltage $V_I - V_S$ was found to be about 5 mV for a V_I as small as 16 mV (Figure 6).

When the illumination of the CdS-containing BLM was continued for a long period, photocorrosion was observed which manifested in the steady decrease of photovoltage. In a typical experiment of 8 h of illumination (with energy of 7 × 10^{-6} W at a wavelength greater than 350 nm), the observed steady-state photovoltage, V_S, decayed almost linearly from an initial value of 165 mV to 88 mV. Over the next 2 h, the decay was much faster, with increasing rate toward the end. Quick occasional monitoring of the dark base line showed a small linear change during the entire course of illumination. The total amount of negative charge (as electrons) transported through the BLM from the trans to cis direction during this 10-h period (the BLM re-

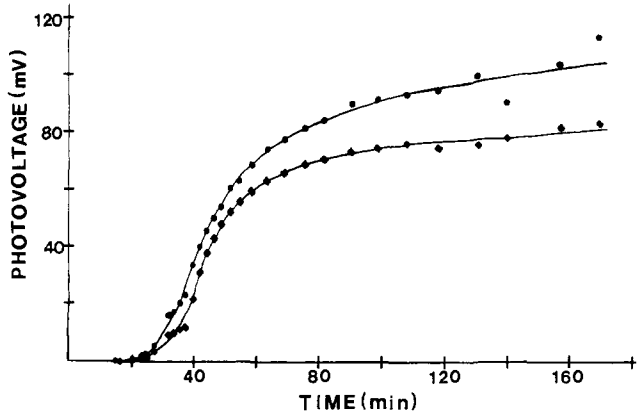

Figure 6. Growth of photovoltage during the formation of CdS particles, in situ, on a GMO BLM. Time was measured from the time of injections of the precursors in the solution bathing the BLM. Initial value, V_I (●), steady-state value, V_S (■).

sistance being 5×10^7 Ω during irradiation) amounted to 1×10^{-4} C. In chemical terms, this corresponded to a change in the concentration of a redox reagent present in the bathing solution on one side by 5×10^{-7} M. The total amount of electrical energy produced by this CdS-containing BLM during the 10-h period was 4×10^{-9} W·h. The largest steady-state charge-transfer quantum yield under these irradiation conditions was found to be only $(3.5 \times 10^{-2})\%$.

Rupture of the BLM at the end of the experiment resulted in the mixing of the cis and trans bathing solutions and in precipitation of CdS. Irradiation of the system after the BLM was ruptured did not produce any photovoltage. Also, control experiments with only GMO BLM (before CdS formation) or without any BLM did not show any photovoltage. In a system containing only a GMO BLM, one of the Ag/AgCl electrodes was deliberately exposed to light by removing its protective sleeve. Irradiation of this electrode produced only a very small photovoltage (<1 mV) as shown in Figure 3 (upper portion). It is interesting to note that the attainment and decay of this small photovoltage signal from electrode irradiation was instantaneous after the light was turned on and off, respectively.

Photovoltage Action Spectra. The action spectra agreed well with the spectrum of bulk CdS (with absorption edge in the 520–530 nm range), indicating that the observed photovoltage is the manifestation of light absorption by the GMO-BLM-incorporated microcrystalline CdS. Irradiation of the hydrocarbon side of the CdS-containing GMO BLM also produced essentially the same action spectra.

Irradiation with Laser Pulses. Excitation of a CdS-containing GMO BLM by 20 ns, 354 nm laser pulses resulted in the buildup of the photovoltage (Figure 7). The direction of the photovoltage was such that the electrode on the cis (CdS) side became negative, as in the steady-state irradiation experiments. The buildup of the photovoltage could be fitted with a single exponential and had a half-life of 235 ± 15 ns.

The decay of the photovoltage signal could be resolved into a faster (completed within 40 μs) and a slower (lasting for 1–2 s) component (see Figure 7). Contribution of the faster process to the overall decay was found to depend on the composition of the system (vide infra).

The photovoltage signal was found to be considerably smaller and shorter lived if the laser-pulse excitation was carried out during the simultaneous steady-state illumination of the sample.

Photovoltage and Photocurrent Measurements as a Function of Load in the External Circuit. Photovoltages generated upon

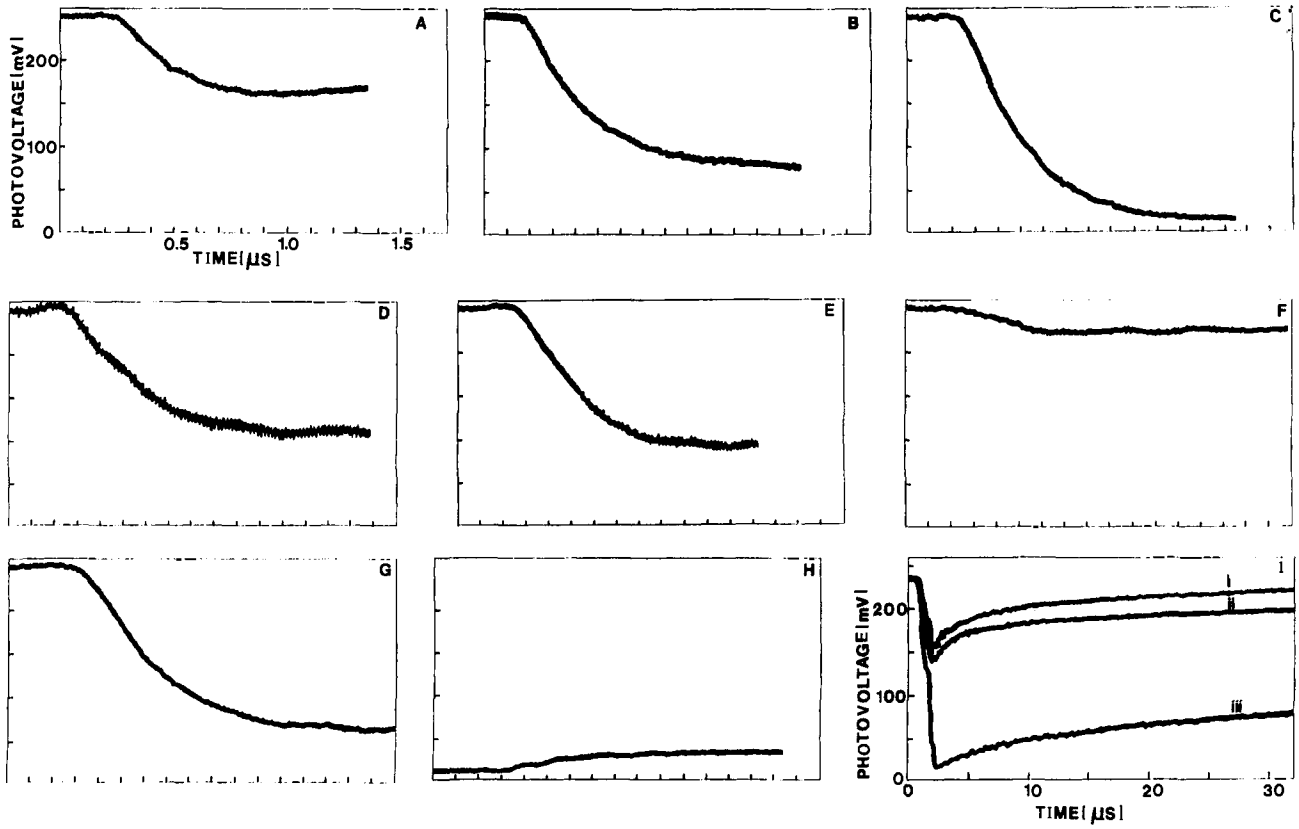

Figure 7. Risetimes of photovoltage signals of a CdS-containing GMO BLM in the absence (A) and in the presence of: 1.0 mM K_2PtCl_6 in the cis side (B); 3.0 mM K_2PtCl_6 in the cis side (C); 5.0 mM $MVCl_2$ in the cis side (D); 10.0 mM $MVCl_2$ in the cis side (E); 13.0 mM D(+)-glucose, 260 μg glucose oxidase, and 130 μg M catalase in the cis side (F); 13.0 mM D(+)-glucose, 260 μg glucose oxidase, 130 μg catalase, and 2.0 mM K_2PtCl_6 in the cis side (G); and 15.0 mM KI_3 in the trans side (H). Buildups were observed by irradiation by 354 nm, 20 ns, 2×10^{-3} mJ laser pulses. The time and voltage scales for all traces are as shown in A. Decays of photovoltage signals of a CdS-containing GMO BLM in the absence (i) and in the presence of: 10 mM $MVCl_2$ in the cis side (ii) and 5 mM K_2PtCl_6 in the cis side (iii). Decays were observed by irradiation by 354 nm, 20 ns, 2×10^{-3} mJ laser pulses.

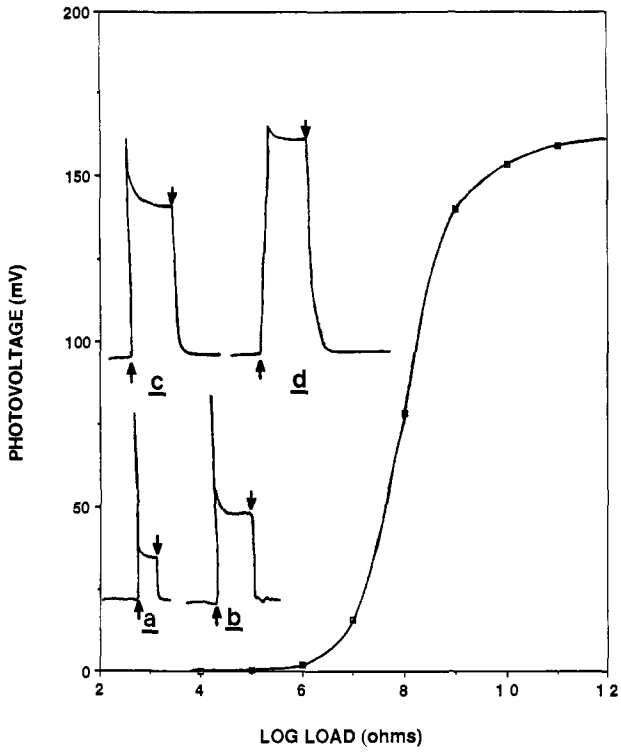

Figure 8. Magnitudes of photovoltage as a function of the load resistance in the external circuit for a CdS-containing GMO BLM while irradiating with $\sim 4 \times 10^{-6}$ W of energy incident on the BLM. The experimental points are connected by a smooth curve for clarity. The insert shows the time evolution of the photocurrent signals when the external resistances were 1×10^7 ohms (a), 1×10^8 ohms (b), 3×10^9 ohms (c), and 1×10^{10} ohms (d). Arrows, ↑ and ↓, indicate the beginning and the termination of the irradiation.

the irradiation of a CdS-containing GMO BLM were determined under conditions of variable current drain (see Experimental Section). A plot of photovoltage against the logarithm of the external resistance is shown in Figure 8. When the external resistance was 10^{10} ohms or higher, the magnitude of the observed photovoltage remained constant and approximated well the value measured under open circuit condition with the electrometer in the voltage measuring mode (156.0 mV). When the external resistance was the same as that of the BLM, i.e. 10^8 ohms, the observed photovoltage was reduced, as expected, to half of its open circuit value. When the external resistance was decreased to a value less than 10^6 ohms, the photovoltage became essentially shorted. Under this condition, the CdS-containing GMO BLM acted as a photocell whose current output changed little with further decrease of resistance in the external circuit. Thus, lowering the external resistance from 10^7 ohms to 10^4 ohms increased the current from 1.5 nA to only 2.0 nA.

Time-dependent variations of the photovoltage signals observed at different load resistances are also illustrated in Figure 8. With increasing value of the load resistance, the initial drop of the voltage signal ($V_1 - V_S$) became progressively smaller and, hence, V_S became greater.

Origin of Photoelectric Effects. Generation of photoelectric effects is best accommodated in terms of light-induced vectorial transfer of charges across the BLM in a direction opposite to the asymmetric BLM potential Φ_m (+426 mV).

Absorption of light quanta with energy larger than 2.6 eV (λ = 530 nm, the bandgap of CdS)[22] results in electron transfer from the valence to the conduction band of the semiconductor:

$$CdS \xrightarrow[\lambda < 530\ nm]{h\nu} e_{CB}^- + h_{VB}^+ \qquad (7)$$

The coincidence of the photovoltage action spectra observed in a CdS-incorporated GMO BLM with the spectrum of bulk CdS semiconductors is in accord with the proposal that eq 7 is responsible for the initiation of the photoevents.

Most of the free carriers, formed in eq 7, undergo quick radiative and nonradiative recombinations at impurity or defect sites. A small number of the electrons ($e_{CB(t)}^-$) and holes ($h_{VB(t)}^+$), however, escape recombination by being trapped both in the bulk and at the surface of the BLM-supported polycrystalline CdS particles. The trapped electrons are transferred, in turn, to oxygen molecules absorbed at the semiconductor–water interfaces, $O_{2(i)}$,

$$O_{2(i)} + e_{CB(t)}^- \rightarrow O_2^{\bullet -}{}_{(i)} \qquad (8)$$

The radical predominantly exists in the form of $O_2^{\bullet -}$ rather than $HO_2^\bullet$ (pK_a = 4.5 for $HO_2^\bullet/O_2^{\bullet -}$). The redox potential of the $O_2/O_2^{\bullet -}$ couple is 0.8 eV lower than the conduction band edge of CdS. Thus, oxygen reduction is a thermodynamically favorable process. Indeed, formation of superoxide radicals ($O_2^{\bullet -}$) during bandgap irradiation of CdS semiconductor particles in oxygenated or aerated aqueous solutions has been well documented.[23,24]

Under the influence of the asymmetric potential, Φ_m (+426 mV) in the CdS-containing GMO BLM (Figure 2), $e_{CB(t)}^-$ will move preferentially to the positive (cis) side and $h_{VB(t)}^+$ will migrate to the negative (trans) side of the membrane. Presence of an asymmetric potential will thus enhance reaction 8 at the cis side of the GMO BLM.

The $O_2^{\bullet -}$ radicals formed at the semiconductor interface are subsequently replaced by oxygen molecules present in the solution, $O_{2(s)}$ either by direct absorption–desorption processes or by electron transfer process as in (9)

$$O_2^{\bullet -}{}_{(i)} + O_{2(s)} \rightarrow O_2^{\bullet -}{}_{(s)} + O_{2(i)} \qquad (9)$$

The removal of an electron from the semiconductor surface to an oxygen molecule in the solution is the net consequence of the processes described by eq 8 and 9.

At the same time, hydrogen sulfide, H_2S, or its dissociated form, SH^- (which are permeable across the BLM and, hence, can approach both of its surfaces), is oxidized by the trapped holes:

$$H_2S + h_{VB(t)}^+ \rightarrow HS^\bullet + H^+ \qquad SH^- + h_{VB(t)}^+ \rightarrow HS^\bullet \qquad (10)$$

Under the influence of the asymmetric potential, the protons will move toward the trans side of the GMO BLM.

Generation of $O_2^{\bullet -}$ in the cis and H^+ (and $^\bullet SH$) in the trans side of the solution bathing the CdS-containing GMO BLM is the net chemical result of bandgap excitation (eq 7–10). Photovoltage decay is the consequence of vectorial recombination of charges, carried by ions (i.e., mass transfer through the BLM), in a direction opposite to the asymmetric membrane potential. Thus, the species formed ($^\bullet SH$, $O_2^{\bullet -}$, and H^+) can either undergo back electron transfer

$$^\bullet SH + O_2^{\bullet -} + H^+ \rightarrow O_2 + H_2S \qquad (11)$$

(which manifests in the decay of the photovoltage signal) or drift apart across the GMO BLM (which is responsible for the long-lived photovoltage signal) under the influence of the asymmetric potential gradient, Φ_m.

Figure 9 illustrates the proposed chemical model compatible with the equivalent circuits, illustrated in Figure 1, b and c, for the generation of photovoltage across the CdS GMO BLM. The magnitude of the photovoltage, V_p, depends on the rate of charge transfer, dQ/dt, across the BLM:

$$V_p = \frac{dQ}{dt} R_m \qquad (12)$$

The observed effects of additives of both steady-state and laser-pulse-initiated photovoltages are in accord with the proposed origin of photovoltaic effects. Thus, removal of oxygen from the

(22) *Landölt Bornstein New Series*; Madelung, O., Ed.; Springer-Verlag: Berlin, 1982; Group III, Vol. 17b, pp 166–194.

(23) Harbour, J. R.; Hair, M. L. *J. Phys. Chem.* **1977**, *81*, 1791–1793.
(24) Harbour, J. R.; Wolkow, R.; Hair, M. L. *J. Phys. Chem.* **1981**, *85*, 4026–4029.

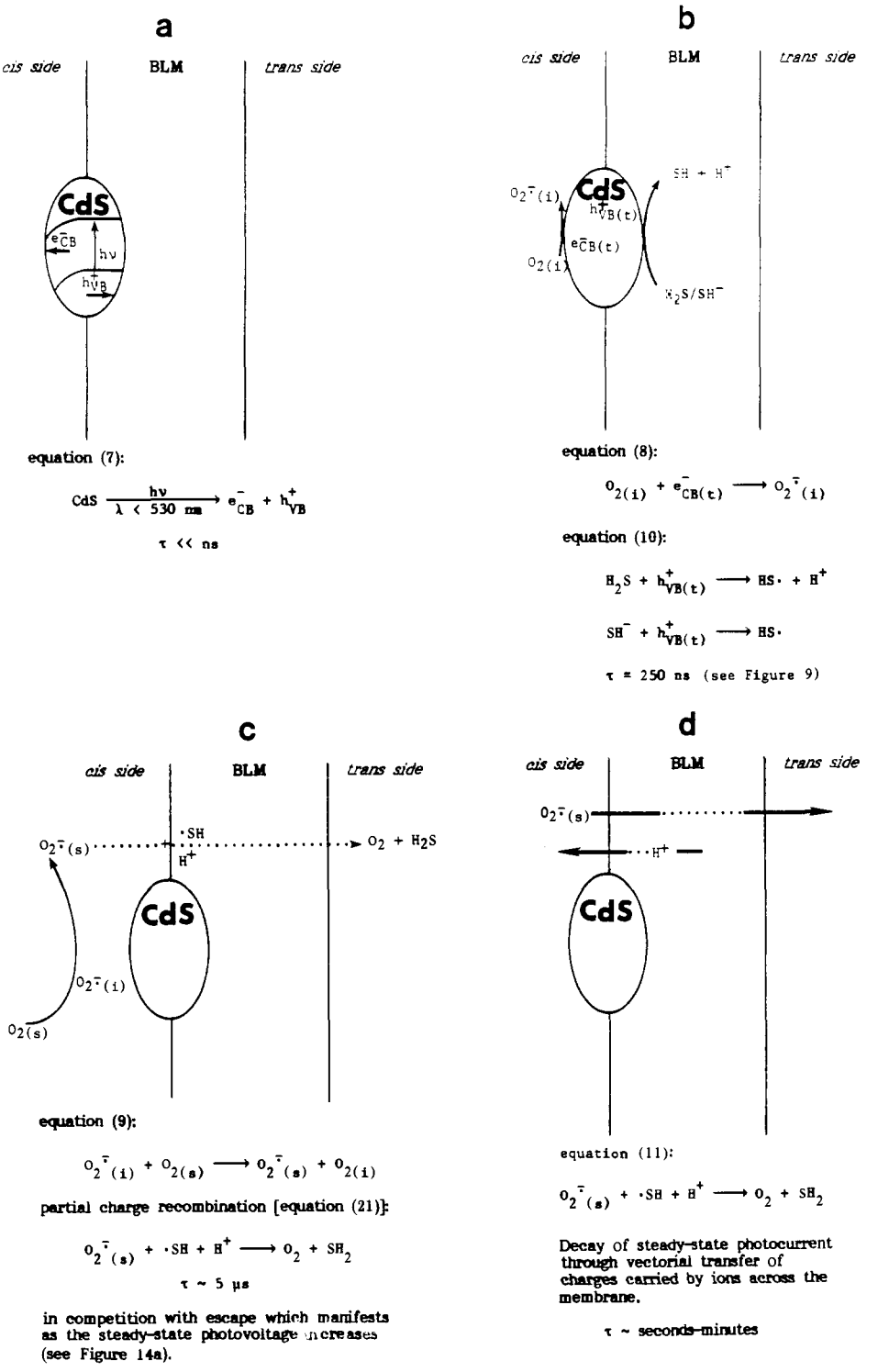

Figure 9. Proposed chemical model for photovoltage generation across the CdS-containing GMO BLM. Reaction sites are highly speculative.

bathing solution by the addition of glucose, glucose oxidase, and catalase[17] drastically reduced both V_I and V_S. The difference $V_I - V_S$ became considerably larger as the rate of oxygen diffusing from the solution to the CdS surface became smaller. The relaxation rate from V_I to V_S however did not seem to change, indicating a true first-order nature, as can be expected from a molecular diffusion process. After a considerably long time (about 4 h), when all of the glucose had been oxidized and the oxygen concentration of the cis bathing solution had increased, again through diffusion from surrounding air, the photovoltage signal was found to regain its original nature and magnitude. Thus, there was no permanent change in the nature of the semiconductor deposit on the BLM by the addition of these enzyme–substrate combinations. Also, control experiments showed that addition of glucose on the cis side of the BLM had no effect on the observed photovoltage. The photovoltage was also found to decrease when the BLM bathing solutions were deoxygenated by using argon gas (although to a somewhat smaller extent than that observed upon the addition of the enzyme–substrate combination). Subsequent to the introduction of oxygen gas into the bathing solution, both V_I and V_S were found to double.

Addition of electron acceptors (MV^{2+} or K_2PtCl_6) to the cis side of the BLM, like that of O_2, aided charge separation (Figure 9). However, addition of $MVCl_2$ (up to 5×10^{-2} M) to the cis side of the BLM resulted only in a small increase [from $-(130 \pm 10)$ mV to $-(175 \pm 10)$ mV] of the observed steady-state photovoltage. On the other hand, the addition of K_2PtCl_6 (3.0×10^{-3} M) or $CuCl_2$ (1.0×10^{-3} M) to the cis side increased the

photovoltage to about 350 mV (with 4 μW of irradiation energy). Electrostatic effects are believed to be responsible for differences in the effects of these two additives. Excess cadmium ions render the GMO BLM supported CdS particles to be positive. Electrostatic attractions favor the diffusion of negatively charged $[PtCl_6]^{2-}$ but hinder the approach of positively charged MV^{2+}. Accordingly, considerably greater photovoltaic effect is observed in the presence of K_2PtCl_6 than that in MV^{2+} at the same concentration. The nature and the shape of the photovoltage signal, as well as the relaxation rates from V_I to V_S, were not appreciably influenced, however, by the addition of K_2PtCl_6 or $CuCl_2$.

As observed in the steady-state experiments, the removal of oxygen, by adding glucose, glucose oxidase, and catalase, resulted in almost complete disappearance of the transient photovoltage signal (Figure 7) on pulsed illumination. When K_2PtCl_6 was added to the cis side of this system, the photovoltage reappeared (Figure 9) with a magnitude similar to that observed with K_2PtCl_6 alone (Figure 7).[20]

Addition of 1–5 mM $KMnO_4$ to the trans side or addition of 1.0 mM $NaHSO_3$ or $Na_2S_2O_5$ to the cis side reduced the magnitude of V_I and V_S. On the other hand, addition of KI_3 to the trans solution bathing the BLM showed a complete reversal of the signs of V_I and V_S. $KMnO_4$ oxidizes the SH^- ion or H_2S to elemental sulfur on the trans side and, thus, reduces the observed photovoltage. $NaHSO_3$ or $Na_2S_2O_5$ competes with the oxidation of SH^- or H_2S. The oxidation of SO_3^{2-} on the cis side of the GMO BLM does not contribute toward the photovoltage and effectively cancels the effect of an equivalent amount of electron transfer to oxygen molecules. Thus, the rate of electron transfer across the BLM and, hence, the observed photovoltage signal are reduced in magnitude, although their relative variation with time remains unchanged. Addition of KI_3 to the trans bathing solution of the BLM, at low concentration, removes the H_2S and SH^- by oxidizing them and thus lowers the magnitude of the observed photovoltage signal. However, when present in high concentrations, KI_3, or I_3^-, which are permeable through the hydrocarbon layer of the BLM, can adsorb at the positive surface of the CdS particles, in preference to oxygen, and thus reverse the vectorial charge transfer. Stating it differently, addition of KI_3 (E° for I_3^-/I^- couple = +534 mV) to the trans side of the CdS-containing GMO BLM is equivalent to applying a larger negative bias potential than Φ_m and consequently to producing a positive photovoltage.

Laser-pulse-initiated photovoltaic effects were also influenced by the presence of additives (Figure 7). In particular, in the absence of additives over 80% of the photovoltage signal generated in the CdS GMO BLM decayed by the fast process. Conversely, if the cis side of the BLM contained 10^{-2} M MV^{2+} and in a separate experiment 5.0×10^{-4} M K_2PtCl_6, contribution of the faster component decreased to ca. 60% and 25%, respectively. Decay of the faster component appeared to follow second-order kinetics: plots of $[V_{(t)} - V_{(40\ \mu s)}]^{-1}$ against time were found to be linear up to 75% of the process. Slopes of these plots were calculated to be 8.35×10^3 and 6.9×10^3 V^{-1} s^{-1} for the CdS-containing GMO BLM in the absence and in the presence of 10^{-2} M MV^{2+}, respectively. Time constants of the slower decay were in the order of the membrane R_mC_m constant (0.1 s).[21]

There are two important consequences of the proposed mechanism. First, the magnitude of the observed photovoltage cannot be greater than the asymmetric BLM potential. This limits the magnitude of observable photovoltage of the CdS-containing GMO BLM to 426 mV in the absence of any external perturbation, such as voltage clamping. Second, under absolutely symmetric conditions (no asymmetric potential of the BLM, no potential drop across the space charge layer in the semiconductor) only a very small photovoltage (~1–2 mV), due to differential $e_{CB(t)}^-$ and $h_{VB(t)}^+$ mobilities—the Dember potential[25]—is expected to develop. Vectorial charge transfer also increases the electrical conductivity and thus contributes to the photoconductance, $1/R_p$.

The rate of electron transfer across the CdS-containing GMO BLM, dQ/dt, is primarily determined by the excess carrier concentration. Thus, eq 12 can be written in terms of the rate constant for the electron transfer (k_e governing eq 8); the extinction coefficient of the semiconductor, K; the recombination lifetime of excess carriers, τ; and the intensity of the incident light, I_0:

$$V_p = k_e K R_m \tau I_0 \qquad (13)$$

Plotting the data according to eq 13 yielded a straight line (insert of Figure 5) whose slope can be equated to $k_eKR_m\tau/h\nu$. An order of magnitude calculation, approximating the irradiating light as a monochromatic one with $\lambda = 400$ nm and using $K = 7 \times 10^5$ cm^{-1},[25] $\tau = 10^{-9}$ s,[27] and $R_m = 6 \times 10^8$ Ω, gives the value of $k_e \sim 10^{12}/cm^3 \cdot s$ from the slope of the insert in Figure 5.

At high illumination intensity, the rate of transmembrane electron transfer becomes limited by the amount of surface adsorbed reactants. Accordingly, at the beginning of the steady-state irradiation, a higher photovoltage, V_I, was observed which quickly relaxed (Figure 3, lower curve) to a lower value of V_S as the surface concentration of the reactant was reduced to a steady-state value. The magnitude of V_S for sufficiently high intensity of light is determined by the rate at which the reactants (O_2, H_2S, or SH^-) are supplied to the CdS particle surface by diffusion from the bulk solution and by the rate which they are consumed by chemical reaction at the interface. Thus, the difference between V_I and V_S becomes greater with increasing light intensity. Below a certain intensity, when the supply rate of the reactant is greater or equal to its depletion rate, $V_I = V_S$ and is determined only by the excess carrier concentration produced by light (eq 13).

The fact that the values of V_I and V_S are respectively determined by the amount of surface absorbed reactants present at the beginning of the irradiation and by the rate of replenishment can also be supported by comparing Figures 5 and 6 (i.e., by considering the dependence of the photovoltage signal on the amount of CdS present in the BLM). V_I is essentially the same as V_S for $V_I < 30$ mV (Figure 5). However, in Figure 6, at the beginning of CdS deposition when the amount of CdS present on the BLM is small, $V_S - V_I$ is quite large (~5 mV) from the very beginning even when V_I is very small (~15 mV).

Dependences of the magnitude and the time variation of the observed photovoltage and photocurrent upon the magnitude of the load resistor present in the external circuit (Figure 8 and insert in Figure 8) can also be rationalized in terms of the proposed model. The photocurrent generated in the absence of any additives is directly proportional to the rate of O_2 reduction in the cis side or to the rate of SH^- or H_2S oxidation in the trans side of the CdS-containing GMO BLM. This, of course, implies that the photovoltage generated is related to the rate of electron transfer across the BLM (eq 13). When the external resistance shorting both sides of the BLM is low (<10^6 ohms), the initial photocurrent drain in the external circuit is high, but it quickly drops to a level determined by the rate of diffusion of the reactants to the surface of the CdS particles and is relatively independent of the magnitude of the external resistance, provided the light intensity is high enough. Conversely, when the external resistance is high (>10^8 ohms) and the current drain in the external circuit is low, the system shows a steady photocurrent from the beginning of the irradiation (i.e., diffusion rate ≥ depletion rate). The effect of external potential, applied across the CdS-containing GMO BLM on the magnitude of the observed photovoltage, is a manifestation of its effect on charge separation. Separations of e_{CB}^- and h_{VB}^+ and/or the products formed from these species are strongly influenced by the presence of the asymmetric potential difference across the CdS-incorporated GMO BLM (~450 mV, Figure 2). An externally applied potential in the same or in the opposite direction may respectively augment or inhibit the photovoltage.

(25) Pankove, J. T. *Optical Processes in Semiconductors*; Dover Publications, Inc.: New York, 1971; p 320.

(26) Gerischer, H. *Angew. Chem., Int. Ed. Engl.* **1988**, *27(1)*, 63–78. Gerischer, H. *NATO ASI Ser.* **1985**, *C146*, 39–106. Kautek, W.; Gerischer, H. *Electrochim. Acta* **1982**, *27(3)*, 355–358. Nosaka, Y.; Fox, M. A. *J. Phys. Chem.* **1988**, *92(7)*, 1893–1897.

(27) Serpone, N.; Pelizzetti, E. In *Homogeneous and Heterogeneous Photocatalysis*; D. Reidel Publishing Company: Dordrecht, Holland, 1986; pp 51–89.

Table I. Photoelectric Effects in CdS-Containing and "Pigmented" BLMS

BLM-forming solution[a]	system[b]			technique	results[c]	ref
glyceryl monooleate (50 mg/mL) in dry decane	5.0 mM KCl, 10 mM $CdCl_2 \rightarrow$ CdS ||		|| 5.0 mM KCl, 12 mM H_2S	excitation by 250 W xenon lamp or 200 W mercury–xenon lamp by 20 ns, 1.2 mJ/cm^2, 354 nm laser pulses, from an Nd–YAG laser	generation of $O_2^{\bullet-}$ in the cis and H^+ in the trans side is the net consequent of bandgap excitation; observed photovoltage is the result of vectorial transfer of charges by ions in the direction opposite to the asymmetric membrane potential; C_p = 2.0–2.2 nF without and 1.5–1.8 nF with CdS; R_m = (3–9) × 10^8 ohms without and (1–8) × 10^8 ohms with CdS; V_I = −150 to −200 mV (cis side negative); V_S = −100 to −140 mV (cis side negative). On turning off illumination potential difference across BLM decreases to dark value	present work
saturated solution of egg lecithin in *n*-octane	10^{-2} M NaCl, 10^{-6} N (A) cyanine dye (D) ||		|| 10^{-2} M NaCl (A)	excitation by 50 W halogen–tungsten lamp or by μs flash lamp	exposure to light results in the prompt developement of photovoltage, V_I = 2 mV (maximum), which quickly decays to zero (i.e., V_S = 0); turning off the light develops a negative photovoltage whose magnitude and decay to 0 mirrors those observed under illumination; photovoltage is the consequence of D^+A^- formation and back electron transfer to DA at one side of the BLM (i.e., no transmembrane e^- transfer) tantamounting to charging and discharging an imaginary capacitor; R_m = 6.2 × 10^8 ohm, C_p = 6 nF	28
egg lecithin (3%), cholesterol (0.8%) in *n*-decane containing also 0.5% chlorophyll *a* (5.5 mM)	0.1 M NaCl, 1 mM (K_2HPO_4 + KH_2PO_4) pH = 6.8, $K_4Fe(CN)_6$, $K_3Fe(CN)_6$ ||	Chl-*a*	|| 0.1 M NaCl, 1 mM (K_2HPO_4 + KH_2PO_4), pH = 6.8	excitation by 0.3 μs, 1–10 mJ, 590 nm laser pulses from a flash lamp pumped Rhodamine 6G dye laser	non-experimental decay of open circuit photovoltage, analyzed in terms of a distribution of rate constants for the reaction of $Fe(CN_6)^{4-}$ with Chl-a^+; C_p = 6–7 nF, R_m = 10^8 Ω, V_S = 2–6 mV	30

[a] Bilayer lipid membranes were typically formed on applying a small quantity of BLM-forming solution across a 1–2 mm diameter hole and subsequent thinning. With a mixture of different lipids, the exact composition of the BLMs may vary quite drastically from that of the BLM-forming solutions. [b] The BLM-containing redox systems are described by vertical pairs of parallel lines. They indicate the planar hydrocarbon–water interface (cis interface on left side, trans on the right) separating two compartments containing aqueous solutions. The region enclosed by the two pairs of parallel lines refers to the membrane core. Membrane soluble species acting as light-absorbing chromophores or as catalysts for electron or proton transfer may be included in this region. Surfactant molecules comprising the bilayer but inert toward light or redox reactions are not indicated. [c] Cp = membrane capacitance, R_m = membrane resistance, V_I = initial photovoltage, developed after irradiation by a steady-state light source, V_S = steady value to which V_I decreases during irradiation.

Disappearance of the photovoltage between −150 and −180 mV of externally applied potential implies that the magnitude of band bending in the semiconductor–electrolyte interface is in the same potential range (150–180 mV).

Conclusion and Comparison to Other Systems

It is instructive to compare the photoelectric behavior of a semiconductor-containing BLM, examined in the present work, with the "pigmented" systems investigated by previous workers.[28-41] Table I facilitates such a comparison for selected systems.

The photosensitizing pigment has been either located on one side of the BLM or freely distributed in the bilayer. Incorporation of a cyanine dye on the cis side of the BLM represents an example of the former system.[19] Exposure to light for a few seconds resulted in the development of a photovoltage which quickly decayed to zero. Immediately after the light was turned off, a negative photovoltage developed whose magnitude and decay to zero mirrored those observed under illumination.[28] In the absence of electron transfer across the BLM, irradiation produced an oxidized dye, D^+, and reduced electron acceptor, A^-, at the BLM interface. With increasingly longer illumination, the observed photovoltage increased until a steady-state concentration of D^+A^- was reached at which point the observed photovoltage attained a maximum. Leakage through the BLM, with a R_mC_m time constant, was responsible for the decay of the photovoltage. The maximum attainable concentration of D^+A^- and, hence, the maximum obtainable photovoltage were determined by the intensity of the irradiation, the concentration and absorption coefficient of the dye, and the rate constants for the rise and decay. Subsequent to turning the light off, the concentration of D^+A^- decreased by back electron transfer, and this decrease produced a photovoltage in the opposite direction. Thus, cyanine dye photosensitized electron transfer at one of the interfaces of the BLM is tantamount

(28) Ullrich, H. M.; Kuhn, H. *Biochim. Biophys. Acta* **1972**, *266*, 584–596.
(29) Feldberg, S. W.; Armen, G. H.; Bell, J. A.; Chang, C. K.; Wang, C. B. *Biophys. J.* **1981**, *34*, 149–163.
(30) Liu, T. M.; Mauzerall, D. *Biophys. J.* **1985**, *48*, 1–7.
(31) Woodle, M.; Zhang, J. W.; Mauzerall, D. *Biophys. J.* **1987**, *52*, 577–586.
(32) Loseu, A.; Mauzerall, D. *Photochem. Photobiol.* **1983**, *38*, 355–361.
(33) Woodle, M. C.; Mauzerall, D. *Biophys. J.* **1986**, *50*, 431–439.
(34) Arrieta, R. T.; Arrieta, I. C.; Pachori, P. M.; Popp, A. E.; Huebner, J. J. *Photochem. Photobiol.* **1985**, *42*, 1–7.
(35) Huebner, J. J.; Arrieta, R. T.; Millar, D. B. *Photochem. Photobiol.* **1982**, *35*, 467–471.
(36) Bienvenue, E.; Seta, P.; Hofmanova, A.; Gavach, C. *J. Electrochem.* **1984**, *162*, 275–284.
(37) Cafioso, D. S.; Hubbell, W. C. *Biophys. J.* **1980**, *30*, 243–264.
(38) Liu, Q. Y.; Tien, H. T. *Photochem. Photobiol.* **1982**, *4*, 73–78.
(39) Hubner, J. J. *J. Membrane Biol.* **1978**, *39*, 97–132.
(40) Vodyanoy, I.; Vodyanoy, V.; Lanyi, J. *Biochim. Biophys. Acta* **1986**, *858*, 92–98.
(41) Hubner, J. S.; Arrieta, R. T.; Arrieta, I. C.; Pachori, P. M. *Photochem. Photobiol.* **1984**, *39*, 191–198.

to charging and discharging an imaginary capacitor.[28] The term "chemical capacitance" has been introduced to describe this capacitance contribution to the observed photovoltage.[8]

Incorporation of CdS into one side of a BLM appears, a priori, to be similar to the incorporation of a cyanine dye. The photoelectric behavior of these two systems is, however, completely different. In the semiconductor-coated BLM, unlike in that covered by the cyanine dye, electron transfer across the bilayer is permitted. Electron transfer products are formed in the solution bathing the opposite sides of the BLM during irradiation, with little depletion of the semiconductor. At the end of irradiation, the steady-state photovoltage simply decays by leakage through the membrane with its characteristic R_mC_m time constant, even though the electron-transfer products are stable in the cis and trans sides of the BLM.

Photoelectrochemistry has been investigated in several systems in which pigments were freely distributed in the BLM.[8,29-34] Chlorophyll and synthetic porphyrin derivatives have been used as pigments, while ferricyanide or MV^{2+} were typically introduced as electron acceptors. Pulsed light irradiation of such a pigmented BLM has resulted in charge separation, due to electron transfer in one of the membrane interfaces. This gave rise to a transient photovoltage signal which decayed as a result of charge recombination. The electron-transfer process for the magnesium octaethylporphyrin pigmented BLM was found to be dynamic; the risetime of the photovoltage signal depended on the concentration of the acceptor ($Fe(CN_6)^{3-}$, MV^{2+}, or anthraquinone-2-sulfonate) present in the bathing solution.[31] This behavior is, of course, very different from that observed in the photoelectrochemistry of the CdS-coated GMO BLM system, studied in the present work. The photovoltage risetime has been found to be independent of the electrolyte concentration (Figure 7), as expected, since the electron transfer occurs on molecules absorbed on the semiconductor surface rather than at the BLM-water interface.

There is also a difference in the decay of the photovoltage signal. In the pigmented BLM, this decay has been found to be long and distinctly non-exponential.[30] The linearity of the plot of V against log T (where T is time elapsed after the pulse) and the insensitivity of the first half-life time on the intensity of the laser pulse is in accord with distributed rate constants arising from different distances (6.5-10 Å) between donors and acceptors at the BLM-water interface. In the CdS-incorporated GMO BLM system, the photovoltage decay followed a much more ideal second-order behavior. This reflects that recombination (eq 11) occurs with a uniform rate constant in a more constrained configuration at the surface of the semiconductor particles. The large magnitude of the observed photovoltage can be attributed to the large asymmetric potential existing across the CdS-containing BLM in our system.

Acknowledgment. Support of this research by the Department of Energy is gratefully acknowledged. We appreciate the critical and thoughtful comments made by the referees on an earlier version of this paper.

Chemical Phenomena in Solid-State Voltammetry in Polymer Solvents

L. Geng,[†] R. A. Reed,[‡] M.-H. Kim,[§] T. T. Wooster, B. N. Oliver,[∥] J. Egekeze,[⊥] R. T. Kennedy, J. W. Jorgenson, J. F. Parcher,[+] and Royce W. Murray*

Contribution from the Kenan Laboratories of Chemistry, University of North Carolina, Chapel Hill, North Carolina 27599-3290. *Received July 5, 1988*

Abstract: This paper, aimed at delineating significant chemical effects in solid-state voltammetry, describes electrochemical oxidations and reductions of electroactive monomer solutes dissolved in and diffusing through rigid and semirigid polymer electrolyte solvents. Sorption of organic monomer vapors into poly(ethylene oxide) films yields polymer solvents whose chemistry is dominated by that of the sorbed monomer as shown by coordination and precipitation effects. The dynamics of plasticization-induced changes in transport rates are quite rapid. Physical diffusion in the polymer solvent in slow enough that electron hopping reactions measurably enhance charge transport rates; the effect was used to estimate a lower limit for the $[Co(bpy)_3]^{2+/+}$ self-exchange rate constant of 2×10^9 M^{-1} s^{-1}. It is possible to erect polymeric film transport barriers at the electrode/polymer solvent interface and to measure the rate of permeation of monomer complexes from the polymer solvent into the polymer transport barrier film. Polymeric films of Os and Ru polypyridine complexes can be electropolymerized from polymer solutions of the corresponding monomers. Solid-state voltammetry can be extended to other polymer solvents including sulfonated polystyrene, poly(vinyl chloride), Nafion, and poly(acrylamide) gel.

This paper describes electrochemical oxidations and reductions of electroactive monomer solutes dissolved in and diffusing through rigid and semirigid polymer electrolyte[1] solvents. The use of polymers as rigid solvents for heterogeneous electron-transfer chemistry is a recent development[2-4] and little is as yet known about this form of solid-state chemistry. This paper describes experiments aimed at delineating significant chemical characteristics of electrochemical reactions in polymeric solutions, including how rigid solvent environments affect rates and mechanisms of electron-transfer reactions and mass transport rates. This paper will also demonstrate how molecular films can be used to

[†] Brookhaven National Laboratories, Upton, NY 11973.
[‡] Dept. of Chemistry, Princeton University, Princeton, NJ 08544.
[§] Dept. of Chemistry, Old Dominium University, Norfolk, VA 23508.
[∥] Laboratory of the Government Chemist, Waterloo Road, London SE18XY.
[⊥] Dept. of Chemistry, Augusta College, Augusta, GA.
[+] Dept. of Chemistry, University of Mississippi, University, MS 38677.

(1) (a) Armand, M. B. *Annu. Rev. Mater. Sci.* **1986**, *16*, 245. (b) Vincent, C. A. *Prog. Solid State Chem.* **1987**, *17*(3), 145. (c) Ratner, M. A.; Shriver, D. F. *Chem. Rev.* **1988**, *88*, 109.

(2) (a) Reed, R. A.; Geng, L.; Murray, R. W. *J. Electroanal. Chem.* **1986**, *208*, 185. (b) Oliver, B. N.; Egekeze, J.; Murray, R. W. *J. Am. Chem. Soc.* **1988**, *110*, 2321. (c) Geng, L.; Reed, R. A.; Longmire, M.; Murray, R. W. *J. Phys. Chem.* **1987**, *91*, 2908. (d) Oliver, B. N.; Egekeze, J.; Murray, R. W., manuscript in preparation.

(3) Geng, L.; Longmire, M. L.; Reed, R. A.; Parcher, J. F.; Barbour, C. J.; Murray, R. W. *Chem. Mater.* **1989**, *1*, 58.

(4) (a) Skotheim, T. A. *Synth. Met.* **1986**, *14*, 31. (b) Skotheim, T. A.; Florit, M. I.; Melo, A.; O'Grady, W. E. *Mol. Cryst.* **1985**, *121*, 291. (c) Skotheim, T. A.; Inganas, O. *Mol. Cryst., Liq. Cryst.* **1985**, *121*, 285. (d) Skotheim, T. A.; Florit, M. I.; Melo, A.; O'Grady, W. E. *Phys. Rev. B* **1984**, *30*, 4846. (e) Inganas, O.; Skotheim, T. A.; Feldberg, S. W. *Solid State Ionics* **1986**, *18/19*, 332. (f) Raleigh, D. O. *Electroanal. Chem.* **1973**, *6*, 87.

0002-7863/89/1511-1614$01.50/0